Archives of Acoustics Online First January 13, 2026 https://doi.org/10.24423/archacoust.2026.4363

Research Paper

Ultrasonic Estimation of Pressure Dependent Non-Linearity Index in Liver

Andrzej Nowicki[(1)*], Jurij Tasinkiewicz[(1)], Piotr Karwat[(1),(2)], Norbert Żołek[(1)], Ihor Trots[(1)], Ryszard Tymkiewicz[(1)]

[(1)] *Institute of Fundamental Technological Research, Polish Academy of Sciences*
Warsaw, Poland

[(2)] *us4us Ltd.*
Warsaw, Poland

*Corresponding Author: anowicki@ippt.pan.pl

Received October 25, 2025; accepted November 14, 2025;
published online January 14, 2026.

This study introduces a proof-of-concept methodology for evaluating pressure-dependent non-linear acoustic properties of liver tissue. The proposed non-linearity index (NLI) is derived from echo amplitudes obtained at two substantially different acoustic pressures. Unlike previous harmonic-based approaches, the method relies solely on the fundamental frequency band, allowing clinical implementation without additional system modifications. The image acquired for the lower pressure is then amplified to correct for the pressure difference between the beams. Next, the NLI is estimated as a ratio of local amplitudes of the amplified low-pressure image (ALPI) to the high-pressure image (HPI). In the case of nonlinear media some energy of the wave is transferred from the pulse fundamental frequency to higher harmonics, which affects mainly the HPI. With the harmonics being filtered out from the signal, the HPI amplitude becomes lower than the ALPI amplitude. As a result, the NLI becomes higher than 1 and increases with the non-linearity of the imaged tissue. The hydrophone measurements were compared to the simulation (k-Wave) of the ultrasonic field in water and vegetable oil. Next, we performed NLI imaging of healthy and fatty livers using SonixTouch (Ultrasonix) systems and two acoustic pressures of 390 kPa and 1590 kPa. Preliminary studies – imaging healthy and fatty livers using SonixTouch (Ultrasonix) systems were performed on the 4 livers of the authors of the article showed that for 'healthy' livers the NLI was below 1.1, while in one of the authors with previously diagnosed steatosis falling between score 1 and 2, the NLI locally exceeded 1.3.

These results show that the obtained NLI values increase with the degree of steatosis, which agrees with theoretical expectations based on tissue B/A coefficients. The work emphasizes methodological feasibility and physical consistency rather than clinical validation, given the limited number of volunteers and ethical restrictions on patient recruitment.

Keywords: ultrasound imaging, abdominal ultrasound, non-linear propagation.

1. Introduction

The scientific goal of the paper is to determine the relationship between the ultrasonic pressure dependent backscattering in liver tissue in vivo in subjects with diagnosed non-alcoholic fatty liver disease (NAFLD) and categorized to the specific steatosis score. An improvement of ability to non-invasively distinguish the fatty tissues will positively affect the specificity and sensitivity of the ultrasound diagnostics of liver. As a result, it will reduce a number of unnecessary biopsies. NAFLD affects 25.24 % of the world's population and 23.71 % of people in Europe, 24.13 % in North America, 30.45 % in South Africa, 31.79 % in the Middle East, and 27.37 % in Asia (Younossi *et al.*, 2016). The NAFLD prevalence of 55 % to 80 % is estimated in patients

with type 2 diabetes (Younossi *et al.*, 2002; 2016; Estes *et al.*, 2018). This results in over 1 billion individuals affected by fatty liver disease worldwide (Saadeh *et al.*, 2002). The problem of NAFLD affects people of all ages, including children, but it may be more pronounced in the elderly population.

About 10 % to 20 % of NAFLD cases are classified as non-alcoholic steatohepatitis (NASH), which must be diagnosed and treated proactively because it can lead to cirrhosis and liver cancer. A liver biopsy is currently the only method that allows for a definitive diagnosis of NASH (Saadeh *et al.*, 2002). However, routine invasive liver biopsy in all patients with such a common disease as NAFLD is unjustified. In the case of the symptoms of liver disease, a liver ultrasound – echogenicity of the liver image and recently the ultrasound attenuation of ultrasound in liver – is a first-choice method of a simple and painless imaging test of liver and its surroundings.

We believe that the implementation of a new ultrasound method for estimating tissue fat content based on the non-linear properties of tissues will provide important additional diagnostic information on the degree of steatosis and will allow for earlier detection of NAFLD, thus improving the prognosis for effective treatment of patients with NAFLD and reducing the need for liver biopsy sampling and testing. The proposed non-linear ultrasound imaging may enable the implementation in clinical practice of a new qualitative signal analysis enabling the assessment of the degree of steatosis.

Up to now, there are four main types of liver ultrasound imaging including:

- B-mode – fatty liver disease might make it brighter, while inflammation might make it denser and darker,
- vascular Doppler ultrasound – exposing the blood flow in liver,
- elastography ultrasound – allowing measuring of the stiffness or fibrosis in liver,
- contrast enhanced ultrasound (CEUS) – allowing for clearer images of liver lesions.

However, studies have shown that although B-mode images alone are useful for assessing steatosis at levels of ≥30 % (Hernaez *et al.*, 2011) they have low sensitivity at lower levels of steatosis (Dasarathy *et al.*, 2009; Bohte *et al.*, 2011). Some development work has been carried out to introduce the transfer learning with a deep convolutional neural network for determination of the hepato-renal index related to the amount of fat in the liver (Byra *et al.*, 2018).

Ultrasound attenuation imaging (ATI) is an emerging method used for detection of hepatic steatosis. It quantifies ultrasound signal attenuation and generates color-coded maps which visualize alterations in liver tissue properties, that may result from changes in hepatic composition (such as increased fat content). The ATI value is defined as dB/cm/MHz. The values increase with increasing levels of steatosis. First studies of the ultrasonic attenuation coefficients of liver have been initiated by Parker *et al.* in 1988. Their results showed that normal attenuation values for the human liver are 0.47 dB/cm/MHz with a frequency-dependent coefficient of 1.05. A trend towards higher attenuation in diffuse liver disease was observed in correlation with increasing fibrosis and fat content, based on liver biopsy grading (Parker *et al.*, 1988). Since then, a numerous reports were published on attenuation in normal and fatty liver (e.g., Tada *et al.*, 2019; Yoo *et al.*, 2020; Hsu *et al.*, 2021; Ferraioli *et al.*, 2022). As for now the guidelines for steatosis score are average (0.52, 0.63, 0.74, and ≥0.78) dB/cm/MHz for S0, S1, S2, and S3, respectively (Jesper *et al.*, 2020; Ogino *et al.*, 2021). The final results differ between research centers using different scanning machines.

Important factors influencing/modifying the measurements of liver attenuation include: respiratory phase, subject positioning, effect of hydration, liver inflammation, subcutaneous fat thickness, scanning technique, frequency dependence attenuation, and bandwidth of the transducer.

We believe that enhancing the currently used algorithm for assessing the degree of steatosis – based on attenuation estimation – by incorporating an independent parameter related to fat-dependent nonlinear propagation of ultrasound in liver tissue, may significantly improve diagnostic accuracy.

The proposed method for assessing the non-linear properties of tissues is, to our knowledge, our original idea, never published before in the world literature.

Modern ultrasound is based on linear and non-linear (tissue harmonic imaging, THI) properties of ultrasound wave propagation in tissue. The basic derivation of the B/A non-linearity coefficient is given in Appendix.

In the field of linear acoustics, particularly in lossless linear media, neglecting wave distortions and the generation of higher harmonics results in $B/A = 0$. In real materials B/A takes finite values. The documented B/A values for some fluids and biological tissue are presented in (Duck, 2002): water (20 °C and 40 °C) $B/A = 4.96$ and 5.38, 3.5 % saline solution (20 °C) $B/A = 5.25$, blood plasma (30 °C) $B/A = 5.74$, whole blood (26 °C) $B/A = 6.1$, fat-free soft tissue $B/A = 6.3$–8.0, and fatty soft tissue $B/A = 9.6$–11.3 (Varray *et al.*, 2010). Dong *et al.* (1999) reported the ultrasonic non-linearity parameter B/A for nine versions of water-based, fat-free and fat-containing, macroscopically homogeneous, ultrasonically tissue-mimicking (TM) materials. The B/A parameter is 1.5 to 2 times larger in adipose tissue than in other tissues, partially explaining the benefits of using harmonic imaging in difficult cases involving excess body fat.

The THI based on acquisitions of the second harmonic components of the ultrasonic echoes was proposed to improve the scanning resolution (van Wijk *et al.*, 2002; Varray *et al.*, 2010). The detection of the nonlinear part of the echoes include different modalities such as: amplitude modulation, pulse inversion or second harmonic inversion (Simpson *et al.*, 1999). THI suffers from lower imaging sensitivity due to the limited frequency bandwidth of available ultrasound transducers. In practice, the lower part of the transducer bandwidth is used in the transmission sequence, while the upper part of the available bandwidth is used during reception and image formation, reducing final imaging sensitivity (Nowicki *et al.*, 2007). The importance of the reduced dynamic range and penetration encountered in THI has also been pointed out (Averkiou *et al.*, 1997; Akiyama, 2000; Averkiou, 2001). THI images are reconstructed solely based on second harmonic components, which results in a reduction of the echo amplitude by more than 20 dB compared to the fundamental components.

A comprehensive review of the estimation of the B/A non-linearity parameter is given in (Panfilova *et al.*, 2021). In addition to the established medical applications of non-linearity, new ultrasound modalities for quantifying the B/A non-linearity parameter (Madigosky *et al.*, 1981) have been continuously developed for several years. Studies on aqueous solutions have shown that the B/A ratio is dependent on the chemical composition and molecular structure of the solutes (Sehgal *et al.*, 1986; Sarvazyan *et al.*, 1990; Gong *et al.*, 2004) and has been found useful for assessing the structure of silicone oil used in ocular surgery (Zhe *et al.*, 2014). It has also been shown to be useful for tissue characterization, showing distinct values for adipose (Law *et al.*, 1985), malignant, healthy, and hepatic tissues in the liver (Errabolu *et al.*, 1988; Panfilova *et al.*, 2021).

It has been shown that B/A is proportional to the change in the speed of sound that accompanies the adiabatic change in pressure. This relation is the basis of the thermodynamic method of measuring B/A (Beye, 1973; Zhu *et al.*, 1983; Zhang, Dunn, 1991; Gong *et al.*, 1993; Everbach, Apfel, 1995; Lu *et al.*, 1998). The finite amplitude method (FAM) exploits the dependence of the speed of sound on B/A and the excess density of the medium (or particle velocity, or excess pressure).

As a consequence of non-linear propagation, the effective attenuation of the wave increases due to the transfer of energy from the fundamental to higher harmonics, which experience stronger attenuation than the fundamental (Coila, Oelze, 2020). In this way, the energy of a high-amplitude non-linear wave is attenuated to a greater extent than the energy of a small-amplitude wave that can be recognized as linear. FAM exploit all these changes, quantifying the distortions by direct observation of the wave profile (Hunter *et al.*, 2016; Takahashi, 1995), by harmonic content (Adler, Hiedemann, 1962; Zhang, Gong, 1999; Fujii *et al.*, 2004; Wallace *et al.*, 2007; Varray *et al.*, 2011) or by observing the non-linearly induced attenuation (Nikoonahad, Liu, 1989; Byra *et al.*, 2017). The FAM approach is relatively simple, though less accurate than the thermodynamic method, carrying potential for clinical applications, enabling B/A tomography for transmission measurements. Recently, Coila *et al.* (2025) proposed a pulse-echo method to estimate B/A based on the theory of the fundamental band amplitude reduction of low amplitude signals.

In this paper we propose a new method for assessing the nonlinear properties of a medium. Our proposal consists in assessing the non-linearity of the medium by comparing echoes from the examined organ using waves that significantly differ in transmitted pressures. In a linear medium, the echo amplitude should be directly proportional to the amplitude of the transmitted signals. The deviation from the linear relationship between the transmitted signal amplitude and the backscatter amplitude depends on the non-linear physical properties of the tissue region being examined. We have developed a method for imaging nonlinear tissue properties that in-

volves comparing signals reflected/scattered in tissues for two or more transmissions that significantly differ in radiated intensity (Nowicki *et al.*, 2024). In tissues with low acoustic non-linearity, ultrasound images will vary in amplitude only proportionally to the amplitude of the transmitted wave. After normalizing echoes proportionally to the amplitude of the transmitted ultrasonic wave, the amplitude ratios of images obtained for low and high sound transmitted pressures should be close to unity. If the examined tissue contains areas with $B/A > 0$, the ratios of subsequent echoes recorded for different transmitted acoustic pressures will differ from unity, and this value should increase with the increasing non-linearity coefficient of the examined tissue. For example, the non-linearity parameter in the liver, adipose tissue, and fatty liver is approximately 7, greater than 8, and close to 11, respectively. This gives hope that this technique can support the diagnosis of fatty liver disease.

The rest of the paper is organized as follows. The following section outlines the proposed method and describes its validation process, which includes experimental measurements and numerical simulations for nonlinear propagation in water and in vegetable oil, as well as liver measurements in-vivo. The results obtained using the proposed method are presented in Sec. 3, while Sec. 4 contains the discussion.

2. Materials and methods

2.1. Method overview

Let us assume that we deal with a linear medium. In such a case, detected echoes would be linearly proportional to the pressure of the transmitted ultrasonic wave. In turn, in the case of a non-linear medium, part of the energy of the propagating wave is transferred from the carrier wave frequency f_0 to higher harmonics $2f_0$, $3f_0$, etc. The energy transfer to higher harmonics increases significantly with the increase in the initial pressure of the transmitted wave scanning the medium. The relative energy transfer to higher harmonics for low pressures of the scanning wave is small compared to this transfer for significantly higher pressures of the scanning wave. As a result, the amplitude of echoes at the fundamental frequency decreases faster with propagation distance for waves transmitted at higher pressures than for those transmitted at lower pressures. We have attempted to use this intuitively simple relationship between the transmission pressure and the rate of energy loss in the fundamental frequency.

Our approach involves acquiring pairs of ultrasound images $E1$ and $E2$, where $E1$ image is obtained using low excitation pressure $P1$, and $E2$ using high pressure $P2$. The reconstruction of these images must rely solely on the fundamental frequency band; higher harmonics should be eliminated – either due to the limited bandwidth of the transducer or through the application of additional low-pass filtering.

The further data processing includes smoothing the $E1$ and$E2$ images using moving average filtration. The final non-linearity index (NLI) image is calculated as the quotient of amplitudes in the 'low pressure' image $E1$ and in the 'high pressure' image $E2$. The echo amplitude ratio for both images is normalized by the factor equal to the transmission pressure ratio for both scans, $P2/P1$:

$$\mathrm{NLI} = \frac{P2}{P1}\frac{E1}{E2}. \tag{1}$$

2.2. Experiments overview

In research (Zhe *et al.*, 2014) the results of experiments conducted in water and in sunflower oil for two different acoustic pressures of 0.39 MPa and 1.55 MPa generated by the ultrasonic head were presented. In-vitro measurements were also performed in a fresh beef liver sample with a small area, into which 1 ml of sunflower oil was injected. Then the course of the NLI was determined in these media. These studies confirmed the correlation between the non-linearity coefficient B/A of the media and the NLI introduced.

In the current work we present results comparing hydrophone measurements in water and sunflower oil with the results of simulations performed in the k-Wave toolbox (Zhu *et al.*, 1983). Subsequently, an in vivo study of the hepatic NLI was conducted on five volunteers, including one with clinically confirmed fatty liver. The three steps leading to the validation od the proposed method are schematically presented in Fig. 1.

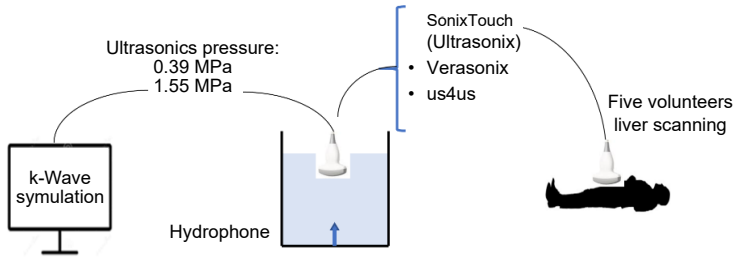

Fig. 1. Schematic diagram of the experimental studies presented in the text.

Throughout our study, a consistent set of excitation signals was employed in both experimental measurements and numerical simulations. We used the 2-cycle tone bursts with a center frequency of 3.3 MHz. The pressure amplitudes $P1$ and $P2$, measured in water at a distance of 1 cm from the transducer surface, were 0.39 MPa and 1.55 MPa, respectively.

2.3. k-Wave simulations

Numerical simulations were performed using k-Wave toolbox (Treeby, Cox, 2010), which is designed for modeling acoustic wave fields in complex media. k-Wave solves the full-wave acoustic propagation equations in the time domain, using FFT-based pseudospectral methods to compute spatial derivatives. This approach offers high accuracy and efficiency, especially for media with smoothly varying properties. The toolbox supports modeling of linear and non-linear wave propagation, frequency-dependent absorption, and heterogeneous media, making it well-suited for comparing propagation in different biological and non-biological environments.

In our simulation study, each medium was modeled by assigning appropriate values of sound speed, density, and absorption (Table 1). The acoustic signal was generated by a focused linear array transducer.

Table 1. Acoustic properties typical for water and vegetable oil.

Medium	Speed of sound [m/s]	Density [kg/m^3]	Absorption [dB/cm/MHz]	Alpha	B/A
Water	1500	1000	0.002	2	6
Vegetable oil	1450	920	0.5	1.8	10

The transducer consists of 32 active elements, each with a width of 480.48 µm (12 grid points), separated by a kerf of 80.08 µm (2 grid points). This gives a pitch of 560.56 µm (14 grid points), and an overall width of approximately 17.86 mm (446 grid points). Each element extends 8.008 mm in elevation (200 grid points), and the focus distance is specified as 20 m, effectively modeling a quasi-plane wave within the near-field of the computational domain, as no explicit time delay laws are applied. The transducer is modeled using k-Wave's function for 3D simulations, allowing control over its aperture, element layout, and elevation profile. Sensors are placed throughout the domain to measure the pressure field, including peak pressure, RMS pressure, and time-varying pressure signals, which are useful for evaluating wavefront shape, focal gain, and attenuation. A 2-cycle tone burst is generated and applied uniformly to all active elements. The simulation is run in 3D, with an input grid size of $1998 \times 462 \times 206$ grid points, representing a physical domain of approximately $80\,\text{mm}^3 \times 18.5\,\text{mm}^3 \times 8.25\,\text{mm}^3$. This domain is embedded within a larger computational grid of $2048 \times 512 \times 256$ points to include perfectly matched layers (PML) and ensures stability. The grid spacing is 30 µm, which provides fine spatial resolution and supports a maximum reliable frequency of 17.73 MHz – well above the 3 MHz center frequency of the source, allowing for accurate modeling of waveform distortion and higher harmonic content generated during nonlinear propagation. The time resolution is equally precise. The simulation uses a time step $\Delta t = 8.4592$ µs, with a total simulation time of 59.9924 µs, covering 7093 time steps. This duration allows sufficient time for the wave to propagate through the domain and interact with the surrounding medium or tissue.

Overall, this simulation setup enables high-fidelity modeling of ultrasound wave propagation through homogeneous or heterogeneous media. It captures essential physical phenomena such as attenuation, dispersion, non-linear distortion, and focusing effects. The fine spatial and temporal resolution, combined with a realistic

source and medium configuration, ensures that the model accurately reflects real-world acoustic wave behavior within the tested soft tissue or fluid environments.

2.4. Hydrophone measurements

The experimental measurements were performed using a needle hydrophone – sensor diameter 0.075 mm (Precision Acoustics, Great Britain). The acoustic excitations were generated using the SonixTouch (Ultrasonix-USA) scanner with a convex probe. The hydrophone measurements were carried out in water and sunflower oil. All the acoustic output parameters were exactly the same as in the k-Wave simulation.

2.5. In-vivo measurements

As a preliminary in-vivo validation of the presented approach, we performed the NLI imaging of healthy and fatty livers (of the authors of this article) using the SonixTouch (Ultrasonix) system. The corresponding mechanical indices MI, calculated for each excitation pulse based on the peak negative pressures measured 1 cm below the transducer face, are given in Table 2. For both applied transmitted pressures, the mechanical index MI was significantly lower than the FDA limit for diagnostic ultrasound, MI < 1.9.

Table 2. MI values for pressures used in the experiments.

Peak to peak pressure [MPa]	Peak negative pressure [MPa]	MI
0.39	0.196	0.11
1.55	0.68	0.37

Standard ultrasound images and backscattered raw radio frequency (RF) echoes up to 14 cm were recorded at the frame rate (RF) of 40. The recording of images for two different pressures was performed as follows. The examination was started for a lower pressure $P1$. After the liver was correctly visualized, a rapid change in the acoustic wave pressure was made by quickly changing the position of the power regulator knob on the scanner control panel.

The $E1$ image was selected from the acquired image sequence as the last frame unaffected by the change in power settings. Similarly, $E2$ was chosen as the first frame in which the amplitude stabilized after the power adjustment. It was experimentally found that the driving voltage applied to the transducer stabilized completely after a time corresponding to three image frames, i.e., after 75 ms (for FR = 40). In such a short time, it is reasonable to assume that the position of the examined liver did not change.

The $E1$ and $E2$ images were subjected to smoothing filtration using 5 mm × 5 mm window. The NLI was calculated according to Eq. (1), and the resulting NLI scan is shown in color scale in Fig. 2.

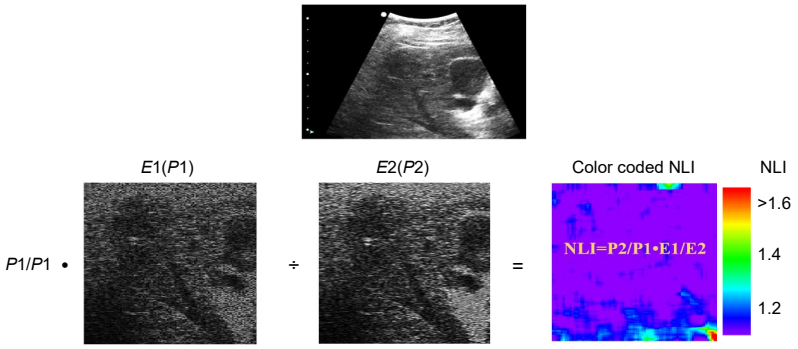

Fig. 2. B-mode image in sector/convex format (top image) is converted to rectangular grid coordinates (bottom images) so that the scan lines are regularly spaced. For each scan, 128 lines are acquired. Both rectangular scans represent the envelope of the raw RF data. The bottom left scan $E1$ is acquired at low transmission pressure $P1$, and after 75 ms the second scan $E2$ (bottom middle) is acquired at high transmission pressure $P2$. NLI color coded scan is shown at bottom right.

3. Results

As stated in the previous section, two experiments were carried out. We measured the first harmonic amplitudes in water and sunflower oil using a needle hydrophone placed at various depths from the face of the convex transducer, from 1 cm to 6 cm. Next the amplitudes of the first harmonic were simulated using k-Wave software. The measurements and simulation were done for two different pressure amplitudes of 0.39 MPa and 1.55 MPa. The results are shown in Fig. 3.

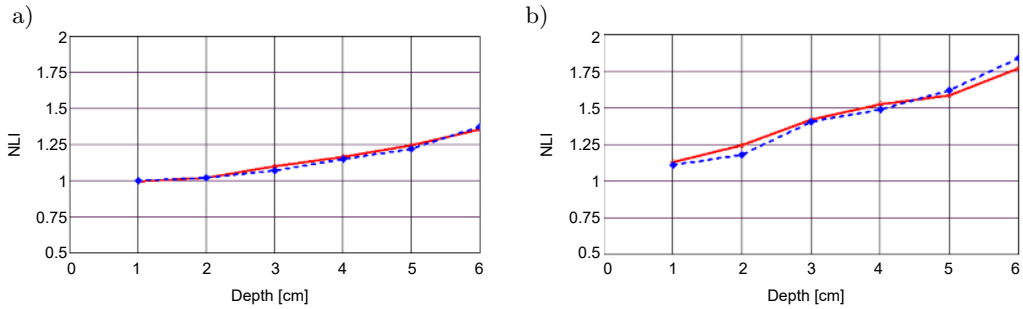

Fig. 3. Plots of NLIs in water (a) and sunflower oil (b), for a pair of acoustic output pressures of 0.39 MPa and 1.55 MPa. Experimental results (solid red lines) are compared with simulation results (dashed blue line).

The NLI scans of four 'healthy' and one fatty liver are shown in Fig. 4. In four imaging studies of 'normal' livers (in Fig. 4a – counting from the top) and one liver with steatosis (Fig. 4b), we determined the mean NLI values and standard deviation (StdDev) at three different depths: 3 cm, 5 cm, and 8 cm counting from the upper

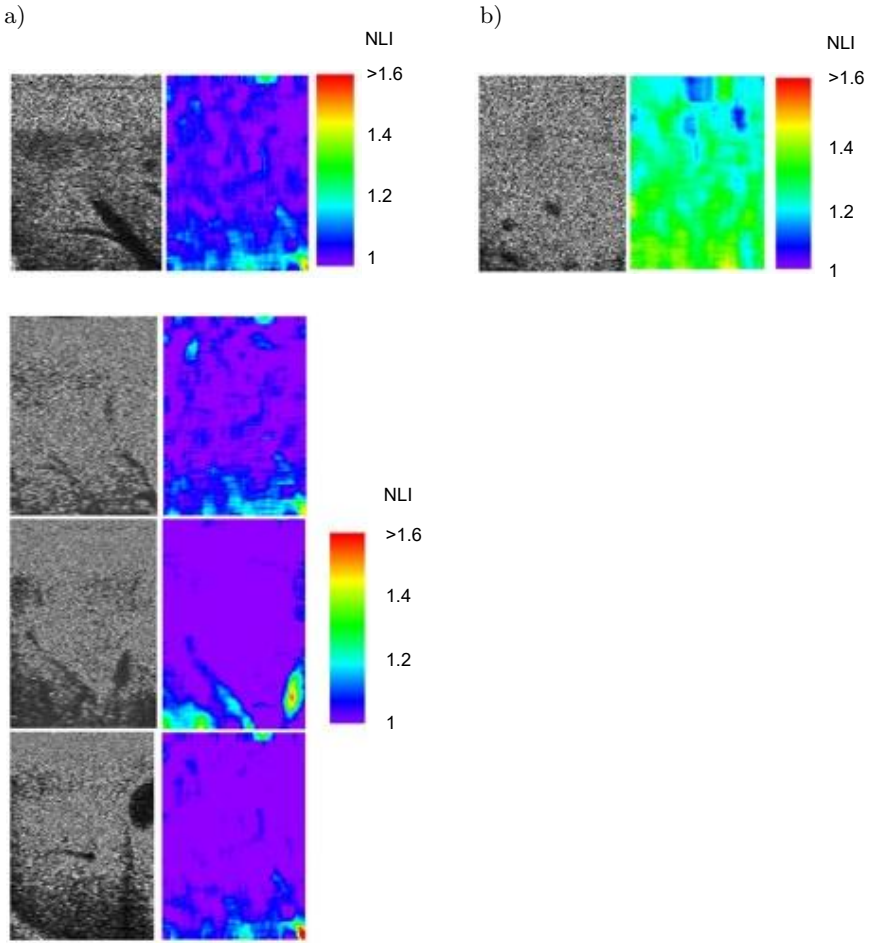

Fig. 4. Preliminary studies on the livers of five authors of the article showed that for 'healthy' livers the NLI was below 1.1 (a), while in one of the authors with previously diagnosed steatosis the NLI locally exceeded 1.3 (b).

border of the liver. The results are presented in Table 3. Both means and StdDev were calculated in 5 mm × 5 mm windows located along the center of the scan.

Table 3. Mean NLI values and standard deviation in scanned livers.

Depth [cm]	Mean StdDev	NLI Liver 1	NLI Liver 2	NLI Liver 3	NLI Liver 4	NLI Liver-steatosis
3	Mean	1.10	1.07	1.09	1.1	1.36
	StdDev	0.03	0.03	0.03	0.03	0.04
5	Mean	1.12	1.09	1.10	1.1	1.4
	StdDev	0.02	0.02	0.025	0.01	0.02
8	Mean	1.11	1.16	1.11	1.15	1.45
	StdDev	0.07	0.03	0.04	0.05	0.03

For healthy volunteers, the mean NLI had values around 1.1, while for the subject with fatty liver it reached 1.45, in agreement with theoretical predictions and simulation data.

4. Discussion

The obtained results confirm the feasibility of the proposed NLI approach for assessing the pressure-dependent nonlinear acoustic response of liver tissue. The method effectively differentiates between healthy and steatotic liver regions using only fundamental frequency information.

Our preliminary results in water, vegetable oil and fatty oil modified beef liver samples presented previously (Zhe *et al.*, 2014) showed clear increase in the NLI in 'fatty' media. The NLI increases faster in oil than in water. This result is in line with expectations, since the non-linearity coefficient B/A is more than 1.5 times higher in oil than in water (water ≈5, vegetable oil >8).

The presented study introduces a novel ultrasound-based NLI for the assessment of pressure-dependent nonlinear properties of liver tissue. We have obtained good convergence between the experimental results and the k-Wave simulations, regarding the amplitude of the first harmonic components of the ultrasound wave propagating in water and sunflower oil.

The simulation results obtained with k-Wave demonstrated the same monotonic dependence of NLI on the nonlinear coefficient (or equivalently B/A), confirming the theoretical expectation that NLI increases with stronger nonlinear behavior.

Preliminary results demonstrate that healthy livers exhibit NLI values around 1.1, while livers with diagnosed steatosis show NLI values exceeding 1.4. This clear distinction highlights the potential of the NLI method as a supportive, non-invasive diagnostic tool for detecting hepatic steatosis. The use of echo signals in the fundamental frequency domain, without reliance on harmonic imaging, further simplifies implementation and adapts well to a variety of clinical ultrasound systems.

Adoption of this approach may significantly enhance the early detection and monitoring of NAFLD, improving patient outcomes and reducing the need for invasive procedures such as liver biopsy.

We are aware that the proposed method has several limitations. Most notably, its outcomes are highly dependent on the imaging depth. Additionally, we estimate that the presence of side-lobes and grating-lobes may significantly affect the results obtained in the NLI mode. These characteristics currently make our method qualitative in nature. In future work, we aim to address these limitations to develop a truly quantitative approach for assessing medium non-linearity. Thanks to the confirmed agreement between the simulations and the measurements, we can support these future efforts with simulations – particularly when attempting acoustic measurements in media with parameters that are difficult to reproduce in laboratory conditions.

In addition to the limitations of the method itself, its validation is constrained by the small sample size – only 5 patients. Consequently, our findings require validation in a considerably larger cohort.

Ongoing and future studies in larger group of patients will be essential to validate the clinical applicability of the pressure-dependent NLI and establish standardized diagnostic thresholds for liver steatosis.

This method opens promising opportunities for quantitative, operator-independent ultrasound diagnostics of liver tissue, potentially setting new standards in non-invasive hepatology.

In summary, the present study should be regarded as a methodological proof-of-concept demonstrating that pressure-dependent analysis of fundamental ultrasound signals can provide reliable insight into the nonlinear behavior of biological tissues.

Further research involving larger patient cohorts and controlled phantom experiments is required to establish calibration between NLI and B/A values and to define diagnostic thresholds for various grades of steatosis.

Appendix

The linear wave equation was derived with three fundamental assumptions:

1. Linearized relationship between pressure and density, $p \cong (\rho - \rho_0)c^2$, where p is acoustic pressure equal to the difference between instantaneous and resting pressure, $p = P - P_0$, ρ_0 is the density of the medium in equilibrium, c is the velocity of longitudinal wave propagation in the medium.
2. Law of conservation of mass $\frac{\mathrm{d}\rho}{\mathrm{d}t} = -\nabla \cdot (\rho v)$, where v is the acoustic particle velocity. This is a nonlinear equation because ρ and v are functions of position variables. The second term is the product of partial velocity and instantaneous density, these are acoustic variables.
3. Euler's equation of motion, $\frac{\mathrm{d}v}{\mathrm{d}t} = -\frac{\nabla p}{\rho}$.

The linearized equation approximates the actual wave propagation only when the speed of sound is much greater than the acoustic particle velocity: $c \gg v$, i.e., when the Mach number M is much smaller than unity, $\mathrm{M} = {}^{v}\!/_{c} \ll 1$. In reality, in the range of applied ultrasonic pressures, i.e., in the range from hundreds of kPascals to MPascals, the tissue volume is compressed and stretched and the speed of sound depends on the pressure. In the equation describing wave propagation, there appears:

1. A nonlinear term describing tissue elasticity (the relationship between pressure and tissue deformation).
2. A nonlinear term related to the deformation of the tissue volume element under the influence of a pressure wave with a strongly distorted / curved wave front. A wave with a finite amplitude propagates slightly faster during positive pressure, when the tissue is compressed and its density increases locally.

Let us assume that the acoustic particle velocity v_0 wave and the wave propagation velocity c have the same direction. If the phases of both waves are the same, then the part of the wave for positive pressure moves faster, with velocity $c_0 + v_0$, while for negative pressure it moves slower, $c_0 - v_0$. For the equation of state $p = f(\rho)$ without linearization, i.e., the assumptions that $p \ll p_0$ and that the changes $\rho - \rho_0$ are negligible, after expanding into a Taylor series, we obtain the expression:

$$p = (\rho - \rho_0)\left(\frac{\partial P}{\partial \rho}\right)_{\rho_0} + \frac{(\rho - \rho_0)^2}{2}\left(\frac{\partial^2 P}{\partial \rho^2}\right)_{\rho_0} + \ldots = A\left(\frac{\rho - \rho_0}{\rho_0}\right) + \frac{B}{2}\left(\frac{\rho - \rho_0}{\rho_0}\right)^2 + \ldots, \tag{2}$$

where $A = \rho_0(\partial P/\partial \rho)_{\rho=\rho_0}$ and $B = \rho_0^2(\partial^2 P/\partial^2 \rho)_{\rho=\rho_0}$.

The ratio B/A is called the non-linearity parameter of the medium. In the linear acoustic regime, where $p \ll P_0$, the changes $\rho - \rho_0$ are very small. Therefore, we can ignore the higher order terms, retaining only $(\rho - \rho_0)$. As a result, we obtain a linear equation:

$$p \approx (\rho - \rho_0)\left(\frac{\partial P}{\partial \rho}\right)_{\rho_0}. \tag{3}$$

The pressure is expressed in Pascals, $1\,\mathrm{Pa} = 1\,\mathrm{N/m^2}$, while the density is expressed in $\mathrm{kg/m^3}$. The quotient of pressure and density has the dimension $(\mathrm{m/s})^2$, i.e., it expresses the velocity in the square, $P/\rho = (\text{velocity})^2$. So,

$$\left(\frac{\partial P}{\partial \rho}\right)_{\rho_0} = c^2. \tag{4}$$

After substituting Eq. (2) describing the nonlinear relationship between pressure and density into Eq. (4) for the wave velocity c_0 and taking into account the convective partial velocity v, we obtain the resultant wave propagation velocity:

$$c = \sqrt{\frac{A}{\rho_0} + \frac{B}{\rho_0}\left(\frac{\rho-\rho_0}{\rho_0}\right) + \ldots} + v = c_0\sqrt{1 + \frac{B}{A}\left(\frac{\rho-\rho_0}{\rho_0}\right) + \ldots} + v. \tag{5}$$

Using the binomial series approximation $(1+x)^n = 1+nx+n(n-1)\frac{x^2}{2!}+\ldots$ we obtain an approximate relationship for the wave velocity in a nonlinear medium:

$$c \cong c_0\left[1 + \frac{B}{2A}\left(\frac{\rho-\rho_0}{\rho_0}\right) + \ldots\right] + v. \tag{6}$$

Taking into account that for a plane wave $\rho c = p/v$ and $p \cong (\rho-\rho_0)\,c^2$, the expression for the velocity in the medium can be written in the form:

$$c \cong c_0 + \frac{B}{2A}v + v = c_0 + \beta v, \tag{7}$$

where

$$\beta = 1 + \frac{B}{2A} \tag{8}$$

is the non-linearity coefficient.

Fundings

This research did not receive any specific grant from funding agencies in the public, commercial, or not-for-profit sectors.

Conflict of interest

The authors declare that they have no known competing financial interests or personal relationships that could have appeared to influence the work reported in this paper.

Authors' contributions

A. Nowicki conceptualized the study and wrote the original draft. A. Nowicki, J. Tasinkiewicz, and P. Karwat developed the experimental setup and performed the analysis and contributed to data interpretation. I. Trots and R. Tymkiewicz performed measurements in vitro. N. Żołek and A. Nowicki performed data processing and simulation. All authors reviewed and approved the final manuscript.

References

1. Adler L., Hiedemann E. (1962), Determination of the nonlinearity parameter B/A for water and m-Xylene, *Journal of the Acoustical Society of America*, **34**(4): 410–412, https://doi.org/10.1121/1.1918142.
2. Akiyama I. (2000), Reflection mode measurement of nonlinearity parameter B/A, *AIP Conference Proceedings*, **524**(1): 321–324, https://doi.org/10.1063/1.1309232.
3. Averkiou M.A. (2001), Tissue harmonic ultrasonic imaging, *Comptes Rendus de l'Académie des Sciences – Series IV – Physics*, **2**(8): 1139–1151, https://doi.org/10.1016/S1296-2147(01)01259-8.
4. Averkiou M.A., Roundhill D.R., Powers J.E. (1997), A new imaging technique based on the nonlinear properties of tissues, [in:] *1997 IEEE Ultrasonics Symposium Proceedings. An International Symposium (Cat. No.97CH36118)*, **2**: 1561–1566, https://doi.org/10.1109/ULTSYM.1997.663294.
5. Beye R.T. (1973), Nonlinear acoustics, *American Journal of Physics*, **41**(9): 1060–1067, https://doi.org/10.1119/1.1987473.

6. Bohte A.E., van Werven J.R., Bipat S., Stoker J. (2011), The diagnostic accuracy of US, CT, MRI and ^{1}H-MRS for the evaluation of hepatic steatosis compared with liver biopsy: A meta-analysis, *European Radiology*, **21**: 87–97, https://doi.org/10.1007/s00330-010-1905-5.
7. Byra M. *et al.* (2018), Transfer learning with deep convolutional neural network for liver steatosis assessment in ultrasound images, *International Journal of Computer Assisted Radiology and Surgery*, **13**(12): 1895–1903, https://doi.org/10.1007/s11548-018-1843-2.
8. Byra M., Wojcik J., Nowicki A. (2017), Ultrasound nonlinearity parameter assessment using plane wave imaging, [in:] *2017 IEEE International Ultrasonics Symposium (IUS)*, pp. 1511–1516, https://doi.org/10.1109/ULTSYM.2017.8092733.
9. Coila A., Oelze M.L. (2020), Effects of acoustic nonlinearity on pulse-echo attenuation coefficient estimation from tissue-mimicking phantoms, *The Journal of the Acoustical Society of America*, **148**(2): 805–814, https://doi.org/10.1121/10.0001690.
10. Coila A., Romero A., Oelze M.L., Lavarello R. (2025), Nonlinearity parameter estimation method from fundamental band signal depletion in pulse-echo using a dual-energy model, *The Journal of the Acoustical Society of America*, **157**(3): 1969–1980, https://doi.org/10.1121/10.0036215.
11. Dasarathy S., Dasarathy J., Khiyami A., Joseph R., Lopez R., McCullough A.J. (2009), Validity of real time ultrasound in the diagnosis of hepatic steatosis: a prospective study, *Journal of Hepatology*, **51**(6): 1061–1067, https://doi.org/10.1016/j.jhep.2009.09.001.
12. Dong F., Madsen E.L., MacDonald M.C., Zagzebski J.A. (1999), Nonlinearity parameter for tissue-mimicking materials, *Ultrasound in Medicine & Biology*, **25**(5): 831–838, https://doi.org/10.1016/s0301-5629(99)00016-2.
13. Duck F.A. (2002), Nonlinear acoustics in diagnostic ultrasound, *Ultrasound in Medicine & Biology*, **28**(1): 1–18, https://doi.org/10.1016/s0301-5629(01)00463-x.
14. Errabolu R.V., Sehgal C.M., Bahn R.C., Greenleaf J.F. (1988), Measurement of ultrasonic nonlinear parameter in excised fat tissues, *Ultrasound in Medicine & Biology*, 14(2): 137–146, https://doi.org/10.1016/0301-5629(88)90181-0.
15. Estes C. *et al.* (2018), Modeling NAFLD disease burden in China, France, Germany, Italy, Japan, Spain, United Kingdom, and United States for the period 2016–2030, *Journal of Hepatology*, **69**(4): 896–904, https://doi.org/10.1016/j.jhep.2018.05.036.
16. Everbach E.C., Apfel R.E. (1995), An interferometric technique for B/A measurement, *The Journal of the Acoustical Society of America*, **98**(6): 3428–3438, https://doi.org/10.1121/1.413794.
17. Ferraioli G., Kumar V., Ozturk A., Nam K., de Korte Ch.L., Barr R.G. (2022), US attenuation for liver fat quantification: An AIUM-RSNA QIBA pulse-echo quantitative ultrasound initiative, *Radiology*, **302**(3): 495–506, https://doi.org/10.1148/radiol.210736.
18. Fujii Y., Taniguchi N., Akiyam I., Tsao J., Itoh K. (2004), A new system for *in vivo* assessment of the degree of nonlinear generation using the second harmonic component in echo signals, *Ultrasound in Medicine & Biology*, **30**(11): 1511–1516, https://doi.org/10.1016/j.ultrasmedbio.2004.08.016.
19. Gong X., Zhang D., Liu J., Wang H., Yan Y., Xu X. (2004), Study of acoustic nonlinearity parameter imaging methods in reflection mode for biological tissues, *The Journal of the Acoustical Society of America*, **116**(3): 1819–1825, https://doi.org/10.1121/1.1781709.
20. Gong X.F., Liu X.Z., Zhang D. (1993), Influences of tissue composition and structural features of biological media on the ultrasonic nonlinearity parameter, *Chinese Journal of Acoustics*, **12**(3): 265–270.
21. Hernaez R. *et al.* (2011), Diagnostic accuracy and reliability of ultrasonography for the detection of fatty liver: A meta-analysis, *Hepatology*, **54**(3): 1082–1090, https://doi.org/10.1002/hep.24452.
22. Hsu P.-K. *et al.* (2021), Attenuation imaging with ultrasound as a novel evaluation method for liver steatosis, *Journal of Clinical Medicine*, **10**(5): 965, https://doi.org/10.3390/jcm10050965.
23. Hunter C. *et al.* (2016), An ultrasonic caliper device for measuring acoustic nonlinearity, *Physics Procedia*, **87**: 93–98, https://doi.org/10.1016/j.phpro.2016.12.015.
24. Jesper D. *et al.* (2020), Ultrasound-based attenuation imaging for the non-invasive quantification of liver fat – A pilot study on feasibility and inter-observer variability, *IEEE Journal of Translational Engineering in Health and Medicine*, **8**: 1800409, https://doi.org/10.1109/JTEHM.2020.3001488.

25. Law W.K., Frizzell L.A., Dunn F. (1985), Determination of the nonlinearity parameter B/A of biological media, *Ultrasound in Medicine & Biology*, **11**(2): 307–318, https://doi.org/10.1016/0301-5629(85)90130-9.

26. Lu Z., Daridon J.L., Lagourette B., Ye S. (1998), A phase-comparison method for measurement of the acoustic nonlinearity parameter B/A, *Measurement Science and Technology*, **9**: 1699–1705, https://doi.org/10.1088/0957-0233/9/10/009.

27. Madigosky W.M., Rosenbaum I., Lucas R. (1981), Sound velocities and B/A in fluorocarbon fluids and in several low density solids, *The Journal of the Acoustical Society of America*, **69**(6): 1639–1643, https://doi.org/10.1121/1.385941.

28. Nikoonahad M., Liu D.C. (1989), Pulse-echo B/A measurement using variable amplitude excitation, [in:] *Proceedings of the 1989 IEEE Ultrasonics Symposium*, pp. 1047–1051.

29. Nowicki A., Tasinkiewicz J., Karwat P., Trots I., Zołek N., Tymkiewicz R. (2024), Ultrasound imaging of nonlinear media response using a pressure-dependent nonlinearity index, *Archives of Acoustics*, **49**(4): 557–563, https://doi.org/10.24425/aoa.2024.148814.

30. Nowicki A., Wójcik J., Secomski W. (2007), Harmonic imaging using multitone nonlinear coding, *Ultrasound in Medicine & Biology*, **33**(7): 1112–1122, https://doi.org/10.1016/j.ultrasmedbio.2007.02.001.

31. Ogino Y., Wakui N., Nagai H., Igarashi Y. (2021), The ultrasound-guided attenuation parameter is useful in quantification of hepatic steatosis in non-alcoholic fatty liver disease, *JGH Open*, **5**: 947–952, https://doi.org/10.1002/jgh3.12615.

32. Panfilova A., van Sloun R.J.G., Wijkstra H., Sapozhnikov O.A., Mischi M. (2021), A review on B/A measurement methods with a clinical perspective, *The Journal of the Acoustical Society of America*, **149**(4): 2200–2237, https://doi.org/10.1121/10.0003627.

33. Parker K.J., Asztely M.S., Lerner R.M., Schenkh E.A., Waag R.C. (1988), In-vivo measurements of ultrasound attenuation in normal or diseased liver, *Ultrasound in Medicine & Biology*, **14**(2): 127–136, https://doi.org/10.1016/0301-5629(88)90180-9.

34. Saadeh S. *et al.* (2002), The utility of radiological imaging in nonalcoholic fatty liver disease, *Gastroenterology*, **123**(3): 745–50, https://doi.org/10.1053/gast.2002.35354.

35. Sarvazyan A.P., Chalikian T.V., Dunn F. (1990), Acoustic nonlinearity parameter B/A of aqueous solutions of some amino acids and proteins, *The Journal of the Acoustical Society of America*, **88**(3): 1555–1561, https://doi.org/10.1121/1.400314.

36. Sehgal C.M., Brown G.M., Bahn R.C., Greenleaf J.F. (1986), Measurement and use of acoustic nonlinearity and sound speed to estimate composition of excised livers, *Ultrasound in Medicine & Biology*, **12**(11): 865–874, https://doi.org/10.1016/0301-5629(86)90004-9.

37. Simpson D.H., Chien T.C., Burns P.N. (1999), Pulse inversion Doppler: A new method for detecting nonlinear echoes from microbubble contrast agents, *IEEE Transactions on Ultrasonics, Ferroelectrics and Frequency Control*, **46**(2): 372–382, https://doi.org/10.1109/58.753026.

38. Tada T. *et al.* (2019), Usefulness of attenuation imaging with an ultrasound scanner for the evaluation of hepatic steatosis, *Ultrasound in Medicine & Biology*, **45**(10): 2679–2687, https://doi.org/10.1016/j.ultrasmedbio.2019.05.033.

39. Takahashi S. (1995), Measurement of acoustic nonlinearity parameter by observation waveforms, *Japanese Journal of Applied Physics*, **34**: 2790–2792, https://doi.org/10.1143/JJAP.34.2790.

40. Treeby B.E., Cox B.T. (2010), k-Wave: MATLAB toolbox for the simulation and reconstruction of photoacoustic wave-fields, *Journal of Biomedical Optics*, **15**(2): 021314, https://doi.org/10.1117/1.3360308.

41. van Wijk M.C., Thijssen J.M. (2002), Performance testing of medical ultrasound equipment: Fundamental vs. harmonic mode, *Ultrasonics*, **40**(1–8): 585–591, https://doi.org/10.1016/s0041-624x(02)00177-4.

42. Varray F., Cachard C., Tortoli P., Basset O. (2010), Nonlinear radio frequency image simulation for harmonic imaging: CREANUIS, [in:] *2010 IEEE International Ultrasonics Symposium*, pp. 2179–2182, https://doi.org/10.1109/ULTSYM.2010.5935538.

43. Varray F., Chenot J., Basset O., Tortoli P., Melodelima D., Cachard C. (2011), Nonlinear parameter imaging to characterize HIFU ablation: Preliminary in vitro results in porcine liver, [in:] *Proceedings of the 2011 IEEE International Ultrasonics Symposium*, pp. 1361–1363, https://doi.org/10.1109/ULTSYM.2011.0336.

44. Wallace K., Lloyd C., Holland M., Miller J.G. (2007), Finite amplitude measurements of the nonlinear parameter B/A for liquid mixtures spanning a range relevant to tissue harmonic mode, *Ultrasound in Medicine & Biology*, **33**(4): 620–629, https://doi.org/10.1016/j.ultrasmedbio.2006.10.008.

45. Yoo J. *et al.* (2020), Reproducibility of ultrasound attenuation imaging for the noninvasive evaluation of hepatic steatosis, *Ultrasonography*, **39**(2): 121–129, https://doi.org/10.14366/usg.19034.

46. Younossi Z.M., Diehl A.M., Ong J.P. (2002), Nonalcoholic fatty liver disease: an agenda for clinical research, *Hepatology*, **35**(4): 746–752, https://doi.org/10.1053/jhep.2002.32483.

47. Younossi Z.M., Koenig A.B., Abdelatif D., Fazel Y., Henry L., Wymer M. (2016), Global epidemiology of nonalcoholic fatty liver disease: Meta-analytic assessment of prevalence, incidence, and outcomes, *Hepatology*, **64**(1): 73–84, https://doi.org/10.1002/hep.28431.

48. Zhang D., Gong X. (1999), Experimental investigation of the acoustic nonlinearity parameter tomography for excised pathological biological tissues, *Ultrasound in Medicine & Biology*, **25**(4): 593–599, https://doi.org/10.1016/s0301-5629(98)00185-9.

49. Zhang J., Dunn F. (1991), A small volume thermodynamic system for B/A measurement, *The Journal of the Acoustical Society of America*, **89**(1): 73–79, https://doi.org/10.1121/1.400370.

50. Zhe Z., Gong C., Dong Z. (2014), Molecular structure dependence of acoustic nonlinearity parameter B/A for silicone oils, *Chinese Physics B*, **23**(5): 054302, https://doi.org/10.1088/1674-1056/23/5/054302.

51. Zhu Z., Roos M., Cobb W.N., Jensen K. (1983), Determination of the acoustic nonlinearity parameter B/A from phase measurements, *The Journal of the Acoustical Society of America*, **74**(5): 1518–1521, https://doi.org/10.1121/1.390154.